Coordination Chemistry of the Soluble Metal Oxide Analogue $[Mo_5O_{13}(OCH_3)_4(NO)]^{3-}$ with Manganese Carbonyl Species

Richard Villanneau, Anna Proust, Francis Robert, and Pierre Gouzerh*[a]

Dedicated to Professor Michel Che

Abstract: The reactions of neutral or cationic manganese carbonyl species towards the oxo-nitrosyl complex $[Na(MeOH)\{Mo_5O_{13}(OCH_3)_4(NO)\}]^{2-}$ have been investigated in various conditions. This system provides an unique opportunity for probing the basic reactions involved in the preparation of solid oxide-supported heterogeneous catalysts, that is, mobility of transition-metal species at the surface and dissolution–precipitation of the support. Under nitrogen and in the dark, the reaction of in situ generated *fac*-$\{Mn(CO)_3\}^+$ species with $(nBu_4N)_2[Na(MeOH)\{Mo_5O_{13}(OMe)_4(NO)\}]$ in MeOH yields $(nBu_4N)_2[Mn(CO)_3(H_2O)\{Mo_5O_{13}(OMe)_4(NO)\}]$ at room temperature, while $(nBu_4N)_3[Na\{Mo_5O_{13}(OMe)_4(NO)\}_2\{Mn(CO)_3\}_2]$ is obtained under reflux. The former transforms into the latter under reflux in methanol in the presence of sodium bromide; this involves the migration of the *fac*-$\{Mn(CO)_3\}^+$ moiety from a basal κ^2O coordination site to a lateral κ^3O site. Oxidation and decarbonylation of manganese carbonyl species as well as degradation of the oxonitrosyl starting material and reaggregation of oxo(methoxo)molybdenum fragments occur in non-deareated MeOH, and both $(nBu_4N)_4[Mn(H_2O)_2\{Mo_5O_{16}(OMe)_2\}_2\{Mn(CO)_3\}_2]$ and $(nBu_4N)_4[Mn(H_2O)_2\{Mo_5O_{13}(OMe)_4(NO)\}_2]$ as well as $(nBu_4N)_2[MnBr\{Mo_5O_{13}(OMe)_4(NO)\}]$ have been obtained in this way. The rhenium analogue $(nBu_4N)_2[Re(CO)_3(H_2O)\{Mo_5O_{13}(OMe)_4(NO)\}]$ has also been synthesized. The crystal structures of $(nBu_4N)_2[Re(CO)_3(H_2O)\{Mo_5O_{13}(OMe)_4(NO)\}]$, $(nBu_4N)_3[Na\{Mo_5O_{13}(OMe)_4(NO)\}_2\{Mn(CO)_3\}_2]$, $(nBu_4N)_4[Mn(H_2O)_2\{Mo_5O_{16}(OMe)_2\}_2\{Mn(CO)_3\}_2]$, $(nBu_4N)_4[Mn(H_2O)_2\{Mo_5O_{13}(OMe)_4(NO)\}_2]$ and $(nBu_4N)_2[MnBr\{Mo_5O_{13}(OMe)_4(NO)\}]$ have been determined.

Keywords: carbonyl ligands · manganese · molybdenum · polyoxometalates · rhenium

Introduction

Polyoxometalates are a rich and diverse class of compounds that are of interest for both fundamental studies and practical applications.[1] The structural analogy between polyoxometalates and extended oxides was first pointed out by Baker[2] and later expanded by Pope,[1a] Klemperer,[3] Finke[4] and Müller.[5] Indeed, the surfaces of many polyanions mimick those of metal oxides, and it is currently thought that the study of transition metal derivatives of polyanions might contribute to the understanding at the molecular level of the different steps of the preparation of heterogeneous metal-oxide-supported catalysts. However polyoxometalate-based transition-metal complexes are not merely analogues of solid oxide-supported catalysts, but they can also display their own catalytic activity. Indeed the polyoxoanion-supported iridium complex $(nBu_4N)_5Na_3[Ir(1,5\text{-cod})P_2W_{15}Nb_3O_{62}]$ has been shown to be an active homogeneous catalyst for the autoxidation of cyclohexene.[6]

The first complexes incorporating an intact polyanion unit were $[M^{IV}(Nb_6O_{19})_2]^{12-}$ (M = Mn, Ni) and $[M^{III}(H_2O)(en)(Nb_6O_{19})]^{5-}$ (M = Cr, Co).[7] Since then organometallic derivatives of the hexametalate ions $[cis\text{-}Nb_2W_4O_{19}]^{4-}$, $[MW_5O_{19}]^{3-}$ (M = Nb, Ta), $[(\eta^5\text{-}C_5H_5)Ti(M_5O_{19})]^{3-}$ (M = Mo, W), and $[(\eta^5\text{-}C_5Me_5)Ti(W_5O_{19})]^{3-}$ have been extensively studied by Klemperer,[8] while triscarbonyl derivatives of the hexaniobate and hexatantalate anions have been recently reported by Pope.[9] Although the free hexavanadate $[V_6O_{19}]^{8-}$ ion is unknown, it can be stabilized through attachement of organometallic groups.[10] Owing to the porphyrin-like nature of metal-substituted polyoanions,[11, 12] monovacant Lindqvist species would be of interest. However, such chemistry has been limited to derivatives of $\{W_5O_{18}\}^{6-}$ until the isolation of the oxonitrosyl species $[Mo_5O_{13}(OMe)_4(NO)]^{3-}$, which can be viewed as a functionalized, monovacant Lindqvist-type polyanion.[13] This species has proved to be a versatile ligand that can act either as a porphyrin-like tetradentate ligand,[13, 14] a bidentate ligand,[15, 16] or a bridging ligand.[15, 17] In addition it may act as

[a] Prof. P. Gouzerh, Dr. R. Villanneau, Prof. A. Proust, F. Robert
Laboratoire de Chimie Inorganique et Matériaux Moléculaires
UMR CNRS 7071, Université Pierre et Marie Curie
case courrier 42, 4 Place Jussieu
75252 Paris Cedex 05 (France)
Fax: (+33) 1-44-27-38-41
E-mail: pg@ccr.jussieu.fr

DOI: 10.1002/chem.200204547

a source of $\{MoO\}^{4+}$ and $\{Mo(NO)\}^{3+}$ units.[16, 18] The formation of $[\{Ni(MeOH)_2\}_2\{Mo(NO)\}_2(\mu_3\text{-}OH)_2(\mu\text{-}OMe)_4\{Mo_5O_{13}(OMe)_4(NO)\}_2]^{2-}$ in the reaction of $(n\mathrm{Bu_4N})_2[Na(MeOH)\{Mo_5O_{13}(OCH_3)_4(NO)\}]$ with various nickel(II) salts in methanol[16] is reminiscent of the dissolution–precipitation of oxide supports in the preparation of supported catalysts.[19] The behavior of $[Na(MeOH)\{Mo_5O_{13}(OCH_3)_4(NO)\}]^{2-}$ towards manganese carbonyls is even more interesting, as it mimicks several of the basic reactions involved in the preparation of supported catalysts by impregnation of oxides with solutions of transition-metal ions, that is, mobility at the surface and dissolution–precipitation of the support. In this account, $[Mo_5O_{13}(OMe)_4(NO)]^{3-}$, for short $\{Mo_5\}$, may be considered as a paradigm for metal oxide analogues in the same way as $[P_2Nb_3W_{15}O_{62}]^{9-}$.[6]

Results

The synthesis and characterization of the following compounds will be discussed: $(n\mathrm{Bu_4N})_2[Na(MeOH)\{Mo_5O_{13}(OMe)_4(NO)\}]\cdot x\,MeOH$ (**1**), $(n\mathrm{Bu_4N})_2[Mn(CO)_3(H_2O)\{Mo_5O_{13}(OMe)_4(NO)\}]$ (**2a**), $(n\mathrm{Bu_4N})_2[Re(CO)_3(H_2O)\{Mo_5O_{13}(OMe)_4(NO)\}]$ (**2b**), $(n\mathrm{Bu_4N})_3[Na\{Mo_5O_{13}(OMe)_4(NO)\}_2\{Mn(CO)_3\}_2]$ (**3**), $(n\mathrm{Bu_4N})_4[Mn(H_2O)_2\{Mo_5O_{13}(OMe)_4(NO)\}_2]$ (**4**), $(n\mathrm{Bu_4N})_2[MnX\{Mo_5O_{13}(OMe)_4(NO)\}]$ X = Br (**5a**), Cl (**5b**), $(n\mathrm{Bu_4N})_4[Mn(H_2O)_2\{Mo_5O_{16}(OMe)_2\}_2\{Mn(CO)_3\}_2]$ (**6**), and $(n\mathrm{Bu_4N})[Mo_2O_5(OMe)_5\{Mn(CO)_3\}_2]$ (**7**).

Syntheses: There is no apparent reaction between **1** and $[MnBr(CO)_5]$ in deaerated methanol at room temperature and in the dark. However, solvated $\{Mn(CO)_3\}^+$, presumably $\{Mn(CO)_3(MeOH)_3\}^+$, formed in situ by treatment of $[MnBr(CO)_5]$ with one equivalent of $AgBF_4$ in MeOH does react with **1** at room temperature. Stirring of a 1:1 mixture of **1** and $\{Mn(CO)_3\}^+$ in MeOH at room temperature for less than 1 h, followed by cooling at $-40\,^\circ C$ for a few days led to the isolation of **2a** in approximately 30% yield. Compound **2a** was also obtained by treating **1** with $\{Mn(CO)_3(MeCN)_3\}^+$[20a] or $[Mn_2Br_2(CO)_6(MeCN)_2]$.[20b] However, the former procedure is preferable due to the instability of **1** in the presence of acetonitrile.[13a] Refluxing of a mixture of **1** with either $\{Mn(CO)_3\}^+$ or $[MnBr(CO)_5]$ in MeOH, followed by cooling at $-40\,^\circ C$ for one week, led to the isolation of **3** in about 54% yield. Compound **3** was alternatively obtained by refluxing a solution of **2a** in MeOH in the presence of NaBr.

In non-deaerated solutions, the reactions of manganese carbonyls towards **1** take a different course. Oxidation and decarbonylation of $\{Mn(CO)_3\}^+$ is indicated by the progressive decrease in the intensity of the band at 390 nm and by the isolation of products containing Mn^{II} centers. Thus compounds **4** and **6** were obtained upon concentration and cooling of solutions of **1** and $\{Mn(CO)_3\}^+$, which had been refluxed first, while **5a** was obtained from a refluxed solution of **1** and $[MnBr(CO)_5]$ in non-deareated methanol. Compounds **4** and **5a** were alternatively obtained upon addition of $Mn(NO_3)_2\cdot 4H_2O$ and $MnBr_2\cdot 4H_2O$, respectively, to a solution of **1** in methanol. Compound **5b** has been similarly obtained from **1** and $MnCl_2\cdot 4H_2O$. It must be noted that **4** is not very stable in methanol and that $(n\mathrm{Bu_4N})_2[Mo_6O_{19}]$ slowly crystallizes from its solutions. The formation of **6** in the course of the reaction of $\{Mn(CO)_3\}^+$ with **1** does not only imply the oxidation and decarbonylation of part of the manganese carbonyl, but also the degradation of $[Mo_5O_{13}(OMe)_4(NO)]^{3-}$ followed by aggregation of oxomethoxo fragments to give the novel lacunary Lindqvist-type $[Mo_5O_{16}(OMe)_2]^{4-}$ ion, which is trapped by $\{Mn(CO)_3\}^+$ and Mn^{II} electrophilic centers. As previously reported,[21] complex **6** can be obtained together with $(n\mathrm{Bu_4N})[Mo_2O_5(OMe)_5\{Mn(CO)_3\}_2]$ (**7**) by refluxing a mixture of $(n\mathrm{Bu_4N})_2[Mo_2O_7]$ and $[MnBr(CO)_5]$ in non-deaerated methanol. However, the most convenient synthesis of **6** consists of adding $(n\mathrm{Bu_4N})_2[Mo_2O_7]$ to a mixture of $Mn(NO_3)_2\cdot 4H_2O$ and $[MnBr(CO)_5]$ in boiling methanol.

The rhenium carbonyl $[ReBr(CO)_5]$ is much less reactive than $[MnBr(CO)_5]$ towards **1**, and no reaction occurs even in boiling MeOH. However, solvated $\{Re(CO)_3\}^+$ slowly reacts with **1** in refluxing MeOH to give **2b**, the rhenium analogue of **2a**. It is noteworthy that the rhenium analogue of **3** was not obtained; this could indicate that $\{Re(CO)_3\}^+$ is much less mobile than $\{Mn(CO)_3\}^+$ at the surface of $[Mo_5O_{13}(OMe)_4(NO)]^{3-}$ (vide infra). In addition $\{Re(CO)_3\}^+$ is much less reluctant than $\{Mn(CO)_3\}^+$ towards oxidation, and no oxidation product was isolated from non-deaerated reacting mixtures.

Spectroscopic characterization: The IR spectra of compounds **2–5** show similar patterns characteristic of the $[Mo_5O_{13}(OMe)_4(NO)]^{3-}$ unit: these are a strong band in the range 1610–1650 cm^{-1} assigned to ν(NO), a fairly broad band of medium intensity in the range 1030–1060 cm^{-1} assigned to the C–O stretches of the methoxo groups, three bands in the range 955–845 cm^{-1} characteristic of terminal oxo groups $\nu(MoO_t)$ and a broad band in the range 670–700 cm^{-1} assigned to ν(Mo-O_b-Mo). According to our previous studies,[14] a three-band pattern for the MoO_t stretches is indicative of a bidentate coordination mode for the $\{Mo_5\}$ ligand, while a two-band pattern is observed when the approximate fourfold symmetry of the ligand is retained upon coordination. A three-band pattern is actually observed for compounds **2** and **4** in accordance with their crystal structures. On the other hand, three bands are also observed for **5a** and **5b**, while only two bands were expected on the basis of the crystal structure of **5a**. However, the two lowest frequency bands are fairly close together. The $\nu(MoO_t)$ band pattern for **3** is unusual, with two weak peaks at 940 and 950 cm^{-1} and a strong one at 911 cm^{-1}. Broadening of the methoxo stretching band arises from the presence of a shoulder on its high frequency side. In addition, the IR spectra of **3** and **6** show low frequency methoxo stretching bands at approximately 1000 cm^{-1}, indicative of triply-bridging methoxo ligands. Assuming local C_{3v} symmetry of the $\{M(CO)_3\}$ groups, one would expect two modes (a_1 and e) in the CO stretching region. The e mode is actually split in the spectra of **2a**, **2b**, **3**, and **6**. The frequencies of the carbonyl bands in **2b** are similar to those of $(n\mathrm{Bu_4N})_3[(Nb_2W_4O_{19})\{Re(CO)_3\}]$,[22] but higher than those of $(n\mathrm{Bu_4N})_8[(P_2W_{15}Nb_3O_{62})\{Re(CO)_3\}]$.[23] This indicates that the $[Mo_5O_{13}(OMe)_4(NO)]^{3-}$ ligand is a donor similar to $[Nb_2W_4O_{19}]^{4-}$, but weaker than $[P_2W_{15}Nb_3O_{62}]^{9-}$. The carbon-

yl bands in **2a** have higher wavenumbers than those of **2b**; this reflects the decreased basicity of manganese with respect to rhenium. On the other hand, there are only minor shifts of the carbonyl bands in **3** and **6** towards **2a**.

The electronic spectra of the triscarbonyl manganese derivatives **2a**, **3**, and **6** display a broad and strong band at approximately 400 nm, which is characteristic of the $\{Mn(CO)_3\}^+$ chromophore.[24] On the other hand, those of **4** and **5b** display a weak band at about 550 nm, which is characteristic of the $[Mo_5O_{13}(OMe)_4(NO)]^{3-}$ unit and was assigned to the $d_{xz},d_{yz} \rightarrow d_{xy}$ transition within the $\{Mo(NO)\}^{3+}$ unit.[13] This band is partly obscured by the $\{Mn(CO)_3\}^+$ transition in the spectra of **2a** and **3**, in which it appears as a shoulder at 535 nm.

The ^1H NMR spectra of **2b** and **3** were recorded at 297 K in [D$_4$]methanol, while the ^{13}C NMR spectra of **2a**, **2b**, and **3** were recorded in methanol/[D$_4$]methanol or methanol/[D$_6$]acetone mixtures. All these spectra display two signals of equal intensity for the methoxo ligands; this is in agreement with the crystal structures of these compounds. At the very least, the ^1H and ^{13}C NMR spectra of **3** indicate that the side-on coordination of the triscarbonyl manganese fragment is retained in solution. In addition, a unique signal was observed at 221.7 ppm for the carbonyl ligands in the ^{13}C NMR spectrum of **2b**, while a 2:1 two-line pattern could be expected on the basis of the crystal structure. That connects with the behavior of the oxotrisalkoxo cluster $[Mo_2O_4\{MeC(CH_2O)_3\}_2\{Mn(CO)_3\}_2]$, whose carbonyl ligands also appear equivalent in solution, but contrasts with that of $[Mo_2O_5(OMe)_5\{Mn(CO)_3\}_2]^-$ and $[Mo_6O_{16}(OMe)_2\{MeC(CH_2O)_3\}_2\{Mn(CO)_3\}_2]^{2-}$.[21] Pivoting of the $\{Re(CO)_3(H_2O)\}^+$ fragment around the lacuna of the $\{Mo_5\}$ ligand would account for the equivalence of the carbonyl ligands in **2b**.

Crystal structures: Compounds **2b**, **3**, **4**, **5a**, and **6** were characterized by single-crystal X-ray diffraction. The selected bond lengths and angles are given in Tables 1 – 5.

Compounds $(n\text{Bu}_4\text{N})_2[Mn(CO)_3(H_2O)\{Mo_5O_{13}(OMe)_4(NO)\}]$ (**2a**) and $(n\text{Bu}_4\text{N})_2[Re(CO)_3(H_2O)\{Mo_5O_{13}(OMe)_4(NO)\}]$ (**2b**) are isomorphous, and only the crystal structure of **2b** was fully analyzed. The molecular structure of the anion of **2b** is displayed in Figure 1. The structure is quite similar to that of $[Cp^*Rh(H_2O)\{Mo_5O_{13}(OMe)_4(NO)\}]^-$.[15] In both cases, the organometallic fragment $\{Cp^*Rh\}^{2+}$ and $\{Re(CO)_3\}^+$, respectively, is bonded to two adjacent axial oxygen atoms of the $\{Mo_5\}$ ligand and achieves an 18-electron configuration through coordination to a molecule of water. In both cases, attachment of the organometallic fragment results in a pattern of bond length alternation. Indeed, the Mo–O bonds that involve the oxygen atoms bonded to rhodium or rhenium, are slightly but significantly lengthened, which results in a shortening of the *trans* Mo–O bonds (Table 1). Also in both cases the water molecule is involved in hydrogen bonds with the two "free" axial oxo ligands of the $\{Mo_5\}$ unit. In **2b**, the distances between these two oxygen atoms (O41 and O51) and the oxygen atom of the coordinated water (O5) are equal to 2.64 and 2.67 Å, respectively. The Re–O bond lengths in **2b** are quite similar to the Rh–O bond lengths in $[Cp^*Rh(H_2O)\{Mo_5O_{13}(OMe)_4(NO)\}]^-$.[15] The differences between the three Re–O bond lengths lie within experimental errors, and it is the same for the three Re–C bond lengths. However, the latter are more spread out (Re1–C4 = 1.79(2), Re1–C3 = 1.85(2), Re1–C2 = 1.89(2) Å); this suggests that the *fac*-$\{Re(CO)_3\}$ unit departs slightly from the ideal C_{3v} symmetry.

The molecular structure of the $[Na\{Mo_5O_{13}(OMe)_4(NO)\}_2\{Mn(CO)_3\}_2]^{3-}$ ion in **3**·MeOH is shown in Figure 2. This species is made of two crystallographically independent $[\{Mo_5O_{13}(OMe)_4(NO)\}\{Mn(CO)_3\}]^{2-}$ units connected by a sodium cation. Each $\{Mn(CO)_3\}^+$ fragment is linked to a distinct $\{Mo_5\}$ unit through the oxygen atoms of two adjacent methoxo ligands and one bridging oxo ligand. The Mn–O bond involving the bridging oxo ligand is only marginally shorter than those with the bridging methoxo ligands. The Mn–C bond lengths are equal within experimental errors

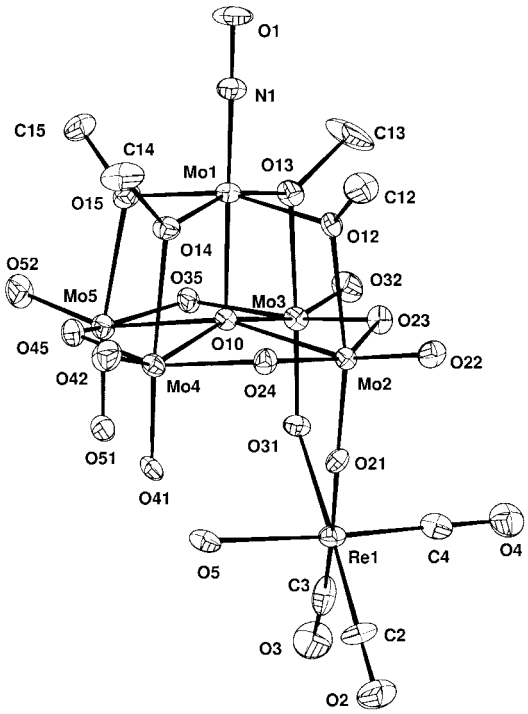

Figure 1. Structure of the anion in **2b** (20% probability thermal ellipsoids).

Table 1. Selected bond lengths [Å] and angles [°] for the anion of **2b**.

O21–Re1	2.130(8)	O31–Re1	2.123(8)
Re1–C2	1.89(2)	Re1–C3	1.84(2)
Re1–C4	1.80(2)	Re1–O5	2.18(1)
C2–O2	1.15(2)	C3–O3	1.20(2)
C4–O4	1.19(2)		
Mo2-O21-Re1	144.2(4)	Mo3-O31-Re1	146.4(5)
O21-Re1-O31	81.2(3)	O21-Re1-C2	96.3(6)
O31-Re1-C2	176.5(6)	O21-Re1-C3	175.7(6)
O31-Re1-C3	94.5(6)	C2-Re1-C3	88.0(8)
O21-Re1-C4	98.7(5)	O31-Re1-C4	93.2(5)
C2-Re1-C4	89.6(7)	C3-Re1-C4	82.3(6)
O21-Re1-O5	80.8(3)	O31-Re1-O5	83.0(3)
C2-Re1-O5	94.2(6)	C3-Re1-O5	98.0(5)
C4-Re1-O5	176.2(5)	Re1-C2-O2	177.3(18)
Re1-C3-O3	172.2(17)	Re1-C4-O4	177.3(13)

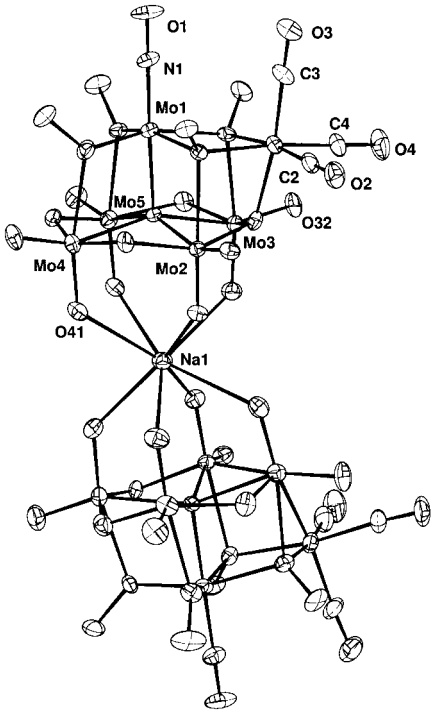

Figure 2. Structure of the complete anion in **3**·MeOH (20% probability thermal ellipsoids). For clarity, only the upper part is labeled.

(Table 2). Although the bonding of the $\{M(CO)_3\}^+$ fragment (M = Mn or Re), and in a general way that of d^6-*fac*-ML_3 fragments, to a triangle of bridging oxygen atoms is usually the rule within polyoxometalate-supported organometallic complexes,[8, 9, 22, 23, 25] such a coordination mode was unknown for the $\{Mo_5\}$ ligand till the characterization of **3**. Each $[\{Mo_5O_{13}(OMe)_4(NO)\}\{Mn(CO)_3\}]^{2-}$ unit interacts with the sodium cation through its four axial oxo ligands in such a way that Na^+ displays distorted square-antiprismatic coordination.

Table 2. Selected bond lengths [Å] and angles [°] for the anion of **3**·CH_3OH.

Mn6–O12	2.062(9)	Mn6–O13	2.075(9)
Mn6–O23	2.024(9)	Mn6–C2	1.78(2)
Mn6–C3	1.80(2)	Mn6–C4	1.78(2)
Mn106–O115	2.07(1)	Mn106–O114	2.066(9)
Mn106–O145	2.021(9)	Mn106–C102	1.78(2)
Mn106–C103	1.80(3)	Mn106–C104	1.81(2)
O2–C2	1.15(2)	O3–C3	1.14(2)
O4–C4	1.15(2)	O102–C102	1.15(2)
O103–C103	1.12(2)	O104–C104	1.13(2)
O12-Mn6-O13	78.9(3)	O12-Mn6-O23	78.6(3)
O13-Mn6-O23	76.2(3)	O12-Mn6-C2	96.0(6)
O13-Mn6-C2	171.6(5)	O23-Mn6-C2	96.2(6)
O12-Mn6-C3	96.8(6)	O13-Mn6-C3	95.9(6)
O23-Mn6-C3	171.5(6)	C2-Mn6-C3	91.4(8)
O12-Mn6-C4	172.6(6)	O13-Mn6-C4	96.9(6)
O23-Mn6-C4	94.6(6)	C2-Mn6-C4	87.4(8)
C3-Mn6-C4	89.7(8)	Mo1-O12-Mn6	101.8(4)
Mo2-O12-Mn6	94.4(3)	Mn6-O12-C12	120.6(8)
Mo1-O13-Mn6	101.4(4)	Mo3-O13-Mn6	95.1(3)
Mn6-O13-C13	117.5(9)	Mo2-O23-Mn6	109.6(4)
Mo3-O23-Mn6	111.0(4)	Mn6-C2-O2	177.9(16)
Mn6-C3-O3	179.1(17)	Mn6-C4-O4	174.9(16)

While seven of the eight Na–O bond lengths lie in a rather narrow range, from 2.53(1) to 2.67(2) Å, the last one is markedky longer (2.83(2) Å). The two square bases of the coordination polyhedron are not strictly parallel, but are at a 8.5° angle. The distortion of the polyhedron could arise from the hydrogen bond between the molecule of methanol and the equatorial terminal oxygen atom O41 (Figure 2).

The molecular structure of the $[Mn(H_2O)_2\{Mo_5O_{16}(OMe)_2\}_2\{Mn(CO)_3\}_2]^{4-}$ ion in **6**·H_2O is shown in Figure 3 (Table 3 give selected bond lengths and angles). This species

Table 3. Selected bond lengths [Å] and angles [°] for the anion of **6**·H_2O.

Mn1–O14	1.99(3)	Mn1–O15	2.09(2)
Mn1–O45	1.99(2)	Mn1–C1	1.79(6)
Mn1–C2	1.76(4)	Mn1–C3	1.76(6)
Mn3–O21	2.13(2)	Mn3–O31	2.16(2)
Mn3–O100	2.18(2)	Mn3–O121	2.17(2)
Mn3–O131	2.12(2)	Mn3–O200	2.21(2)
Mn101–C102	1.72(4)	Mn101–O114	2.06(2)
Mn101–O115	2.04(2)	Mn101–O145	2.06(2)
Mn101–C101	1.82(4)	Mn101–C103	1.66(4)
O1–C1	1.11(6)	O2–C2	1.18(4)
O3–C3	1.13(5)	O101–C101	1.07(4)
O102–C102	1.20(4)	O103–C103	1.27(4)
O14-Mn1-O15	75.1(9)	O14-Mn1-O45	77.6(9)
O15-Mn1-O45	78.2(8)	O14-Mn1-C1	99.7(19)
O15-Mn1-C1	98.7(20)	O45-Mn1-C1	176.3(19)
O14-Mn1-C2	98.1(15)	O15-Mn1-C2	172.1(14)
O45-Mn1-C2	96.6(14)	C1-Mn1-C2	86.3(22)
O14-Mn1-C3	169.5(18)	O15-Mn1-C3	98.6(18)
O45-Mn1-C3	93.1(18)	C1-Mn1-C3	89.4(24)
C2-Mn1-C3	87.6(20)	O21-Mn3-O31	87.2(8)
O21-Mn3-O100	93.6(9)	O31-Mn3-O100	88.8(9)
O21-Mn3-O121	178.8(9)	O31-Mn3-O121	93.3(9)
O100-Mn3-O121	87.5(9)	O21-Mn3-O131	92.8(9)
O31-Mn3-O131	179.4(9)	O100-Mn3-O131	91.8(9)
O121-Mn3-O131	86.7(9)	O21-Mn3-O200	89.8(9)
O31-Mn3-O200	86.7(9)	O100-Mn3-O200	174.3(10)
O121-Mn3-O200	89.2(9)	O131-Mn3-O200	92.7(9)
Mn1-O14-Mo1	105.9(11)	Mn1-O14-Mo4	95.8(9)
Mn1-O14-C14	121.2(19)	Mn1-O15-Mo1	104.9(10)
Mn1-O15-Mo5	94.0(8)	Mn1-O15-C15	115.5(19)
Mn3-O21-Mo2	140.7(13)	Mn3-O31-Mo3	138.5(12)
Mn1-O45-Mo4	111.4(10)	Mn1-O45-Mo5	108.5(10)
Mn1-C1-O1	171.4(55)	Mn1-C2-O2	176.4(37)
Mn1-C3-O3	169.0(48)		

can be viewed as being made of two crystallographically independent $[\{Mo_5O_{16}(OMe)_2\}\{Mn(CO)_3\}]^{3-}$ units connected by a $\{Mn(H_2O)_2\}^{2+}$ linker. The features of the $[\{Mo_5O_{16}(OMe)_2\}\{Mn(CO)_3\}]^{3-}$ units in **6**·H_2O are quite similar to those of the $[\{Mo_5O_{13}(OMe)_4(NO)\}\{Mn(CO)_3\}]^{2-}$ units in **3**. Each $\{Mn(CO)_3\}^+$ fragment is linked to a distinct $[Mo_5O_{16}(OMe)_2]^{4-}$ ligand through the oxygen atoms of the methoxo ligands and one bridging oxo ligand. The novel lacunary Lindqvist-type isopolyanion $[Mo_5O_{16}(OMe)_2]^{4-}$ derives from $[Mo_5O_{18}]^{6-}$ through the replacement of two adjacent side-on bridging oxo ligands by methoxo ligands. Both species remain unknown when uncomplexed. Besides side-on coordination to a $\{Mn(CO)_3\}^+$ cation, each

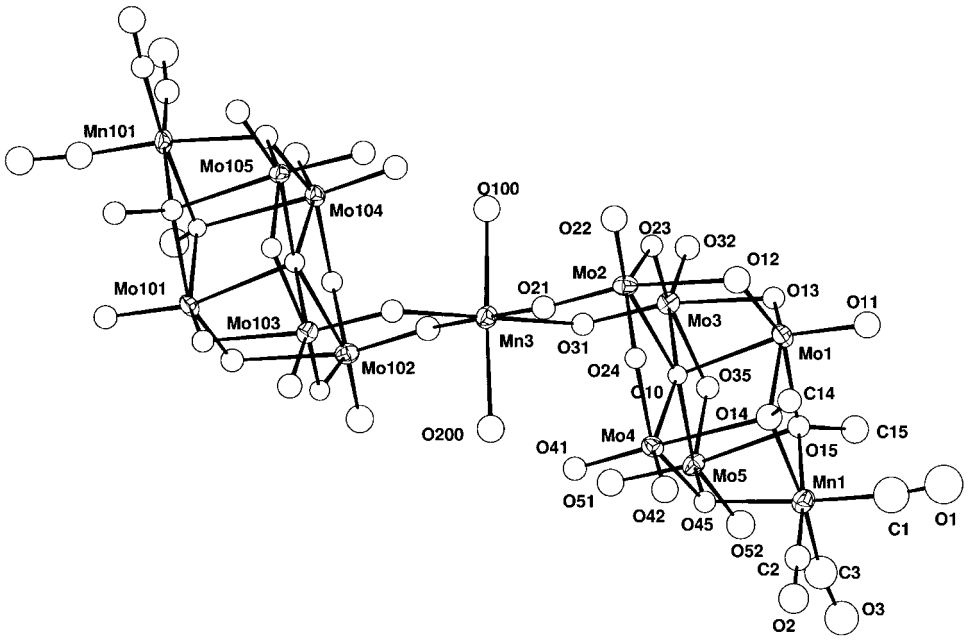

Figure 3. Structure of the anion in $\mathbf{6}\cdot H_2O$ (20% probability thermal ellipsoids).

$[Mo_5O_{16}(OMe)_2]^{4-}$ acts as a bidentate ligand towards the Mn^{II} center, which achieves octahedral coordination with two mutually *trans* molecules of water. It is unlikely that lacunary Lindqvist-type polyanions such as $[Mo_5O_{16}(OMe)_2]^{4-}$ and $[Mo_5O_{18}]^{6-}$ would display side-on coordination unless the oxo ligands that delineate the lacuna are already bonded to some electrophilic fragment. Further examples are provided by the recently reported clusters $[Ru(\eta^6\text{-}C_6Me_6)(H_2O)(M_5O_{18})\{Ru(\eta^6\text{-}C_6Me_6\}_2]$ (M = Mo, W), which can be viewed as $[M_5O_{18}]^{6-}$ polyanions supporting one $\{Ru(\eta^6\text{-}C_6Me_6)(H_2O)\}^{2+}$ and two $\{Ru(\eta^6\text{-}C_6Me_6)\}^{2+}$ fragments.[27] When two different electrophilic groups are involved, as in **3** and **6**, hard cations, such as Na^+ and Mn^{2+}, show preference towards the oxygen atoms of the lacuna.

The structure of the centrosymmetrical $[Mn(H_2O)_2\{Mo_5O_{13}(OMe)_4(NO)\}_2]^{4-}$ ion in **4** is shown in Figure 4 (selected bond lengths and angles are given in Table 4). As far as Mn^{II} center is concerned, the molecular structures of the anions in **4** and **6** are quite similar. In $[Mn(H_2O)_2\{Mo_5O_{13}(OMe)_4(NO)\}_2]^{4-}$, the Mn^{II} center is linked to two bidentate $\{Mo_5\}$ ligands and achieves octahedral coordination with two molecules of water. The coordination mode of the $\{Mo_5\}$ ligand is the same as in **2**, and the O···O distances of 2.78 and 2.80 Å are indicative of hydrogen bonding between the coordinated water molecules and the axial oxygen atoms of the polyanions that are not bonded to Mn^{II}.

The molecular structure of the complex $[MnBr\{Mo_5O_{13}(OMe)_4(NO)\}]^{2-}$ in **5a** is displayed in Figure 5 (selected bond lengths and angles are given in Table 5). The Mn^{II} center exhibits square-pyramidal pentacoordination and is displaced by 0.83 Å from the plane of the four oxygen donors towards the apical bromide ligand. Furthermore, the Mn–Br bond is not exactly orthogonal to the basal plane of the pyramid. Indeed two of the O-Mn-Br angles are close to 109°, while the other two are close to 116°. The Mn–O bond lengths are similar to those in compounds **4** and **6**. In contrast to compounds **2** and **4**, in which a pattern of bond length alternation is clearly apparent within the $\{Mo_5\}$ ligand, a symmetrical pattern is observed in **5a**; this reflects the symmetrical coordination mode.

Discussion

Triscarbonylmanganese(I) complexes and their rhenium analogues have played a key role in the development of organometallic chemistry of polyoxometalates. Indeed the complexes $[(OC)_3M(Nb_2W_4O_{19})]^{3-}$ (M = Mn, Re) were the very first polyoxometalate-supported organometallic complexes to

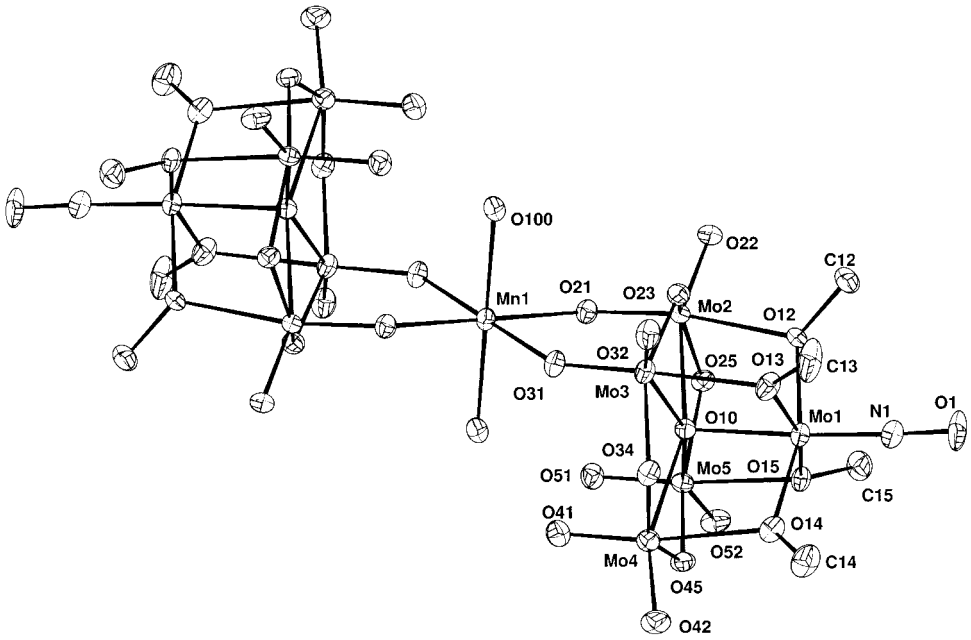

Figure 4. Structure of the centrosymmetrical anion in **4** (20% probability thermal ellipsoids).

Table 4. Selected bond lengths [Å] and angles [°] for the anion of **4**.

Mn1–O21	2.201(6)	Mn1–O31	2.150(6)
Mn1–O100	2.188(7)	Mn101–O131	2.154(7)
Mn101–O151	2.161(6)	Mn101–O200	2.204(7)
O21-Mn1-O31	84.7(2)	O21-Mn1-O31′	95.3(2)
O21-Mn1-O100	93.7(3)	O31-Mn1-O100	94.0(3)
O21-Mn1-O100′	86.3(3)	O31-Mn1-O100′	86.0(3)
Mo2-O21-Mn1	141.0(4)	Mo3-O31-Mn1	142.7(4)
O131-Mn101-O151	84.5(2)	O131-Mn101-O151′	95.5(2)
O131-Mn101-O200	91.7(3)	O131-Mn101-O200′	88.3(3)
O151-Mn101-O200	91.6(3)	O151-Mn101-O200′	88.4(3)
Mo103-O131-Mn101	141.7(4)	Mo105-O151-Mn101	142.8(4)

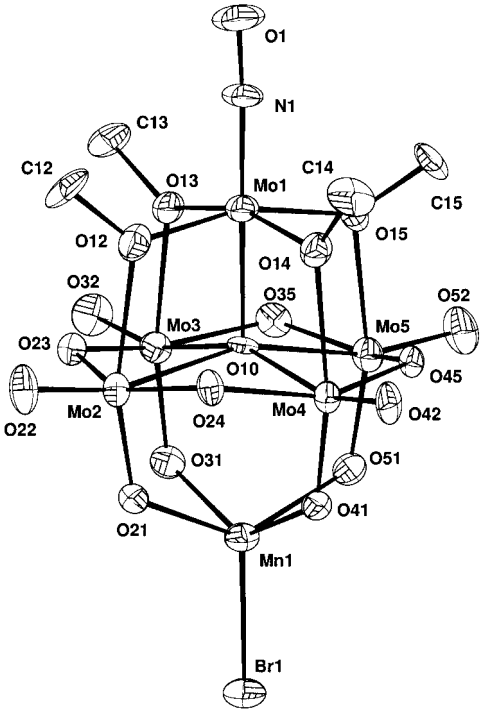

Figure 5. Structure of the anion in **5a** (20% probability thermal ellipsoids).

Table 5. Selected bond lengths [Å] and angles [°] for the anion of **5a**.

Mn1–Br1	2.457(3)	Mn1–O21	2.16(1)
Mn1–O31	2.14(1)	Mn1–O41	2.18(1)
Mn1–O51	2.14(1)		
Br1-Mn1-O21	116.2(3)	Br1-Mn1-O31	108.9(3)
O21-Mn1-O31	81.7(4)	Br1-Mn1-O41	116.1(3)
O21-Mn1-O41	81.0(4)	O31-Mn1-O41	134.9(4)
Br1-Mn1-O51	109.1(3)	O21-Mn1-O51	134.6(4)
O31-Mn1-O51	81.7(4)	O41-Mn1-O51	81.6(4)

be reported,[22] followed by the $\{Mn(CO)_3\}^+$ adduct of the $[Mo_5O_{18}(TiCp)]^{3-}$ ion.[25] Derivatives of the Dawson-type $[P_2W_{15}Nb_3O_{62}]^{9-}$ polyoxoanion[23] and of the Lindqvist-type hexametalate anions, $[M_6O_{19}]^{8-}$ (M = Nb, Ta),[9] have been more recently reported. In all these complexes the metal triscarbonyl unit is bonded to a triangle of three bridging oxygen atoms. A different binding mode is observed in $[M(CO)_3(H_2O)\{Mo_5O_{13}(OMe)_4(NO)\}]^{2-}$ (M = Mn, Re), in which the metal triscarbonyl unit is bonded to two terminal oxygen atoms of the polyanion and to a molecule of water. To the best of our knowledge, the polyanion acts as a tridentate ligand in all previously reported complexes of plenary polyoxometalates with *fac*-d^6-$\{ML_3\}$ units, such as $\{M(CO)_3\}^+$,[8, 9, 22, 23, 25] $\{Rh(\eta^5\text{-}C_5Me_5)\}^{2+}$,[3, 8, 26, 28a,b] and $\{Ru(\eta^6\text{-arene})\}^{2+}$,[10c, 28] with the possible exception of $[Cp^*RhCl_2(Nb_2W_4O_{19})]^{4-}$, which has been proposed as an intermediate in the formation of $[Cp^*Rh(Nb_2W_4O_{19})]^{2-}$ by reaction of $[Cp^*RhCl_2]_2$ with $[Nb_2W_4O_{19}]^{4-}$, and in which the polyanion is assumed to bind to rhodium through one of its ONb oxygen atoms.[26a] We anticipated the defect $[Mo_5O_{13}(OMe)_4(NO)]^{3-}$ ion binding through the oxygen atoms that delineate the lacuna. Indeed its adducts with *fac*-d^6-$\{ML_3\}$ fragments usually display κ^2O coordination, and the complexes $[M(CO)_3(H_2O)\{Mo_5O_{13}(OMe)_4(NO)\}]^{2-}$ (M = Mn, Re) and $[Cp^*Rh(H_2O)\{Mo_5O_{13}(OMe)_4(NO)\}]^{-}$[15] are isostructural.

However, the manganese adduct is unique in that migration of the triscarbonyl manganese unit can be induced by Na^+ ions. Indeed, compound **2a** is obtained from the reaction of **1** with solvated $\{Mn(CO)_3\}^+$ ions at room temperature, while **3** is obtained upon heating. Moreover, compound **3** can be obtained upon heating a solution of **2a** in MeOH in the presence of a sodium salt. These observations suggest that **2a** is the kinetic product of the reaction, while **3** is the thermodynamic product. Of direct relevance to the present work, is the Dawson-type polyoxoanion-supported $\{Re(CO)_3\}^+$ complex $[\{Re(CO)_3\}(P_2W_{15}Nb_3O_{62})]^{8-}$, which displays either non-C_{3v} or C_{3v} symmetry depending on whether sodium cations are present or not.[23] Only a few other examples of isomerization processes involving organometallic cation mobility on polyoxoanions have been reported. These are the intermolecular isomerization of $[Cp^*Rh(Nb_2W_4O_{19})]^{2-}$, which involves the $[(Cp^*Rh)_2(Nb_2W_4O_{19})]$ molecule as an intermediate,[26a] the intramolecular *endo*–*exo* isomerization of the vanadate-supported complexes $[\{(\eta^4\text{-}C_8H_{14})Rh\}_2(V_4O_{12})]^{2-}$ and $[\{(\eta^4\text{-}C_6H_{10})Rh\}_2(V_4O_{12})]^{2-}$ through pivoting of the organometallic fragments on the surface of the metavanadate ring,[29] and the intramolecular windmill-triple cubane isomerization of the cluster $[\{Ru(\eta^6\text{-}p\text{-}MeC_6H_4iPr)\}_4Mo_4O_{16}]$.[30] Besides these processes with net structural changes, organometallic cation mobility could also account for the fluxional behavior of some polyoxoanion-supported organometallic complexes, in particular those containing $\{Ir(\eta^4\text{-}C_8H_{12}\}^+$ groups.[31] Nevertheless, examples of organometallic cation mobility over a polyoxoanion surface are still rare. They are, however, of interest as models in oxide-supported organometallic chemistry as there is evidence for the mobility of surface intermediates.[32]

Another significant feature of the $[Mo_5O_{13}(OMe)_4(NO)]^{3-}$ ligand is its ability to transform under various conditions. Indeed, this polyanion is only fairly stable and can act as a source of both $\{Mo(NO)\}^{3+}$ and $\{MoO\}^{4+}$ moieties. In CH_2Cl_2 or MeCN, reaggregation yields the $[Mo_6O_{18}(NO)]^{3-}$ ion,[13a] while the moiety can be trapped by the monovacant Keggin-type polyoxometalates $[PM_{11}O_{39}]^{7-}$ to give $[PM_{11}O_{39}\{Mo(NO)\}]^{4-}$ (M = Mo, W).[18a] In the presence of Ni^{II} salts, limited decomposition of $[Mo_5O_{13}(OMe)_4(NO)]^{3-}$

occurs and subsequent reaggregation leads to the formation of a rhomblike Ni_2Mo_2 cluster, which is stabilized by coordination to two $[Mo_5O_{13}(OMe)_4(NO)]^{3-}$ units.[16] This reaction is reminiscent of the reactions of dissolution – reprecipitation of oxides by reaction with metal ions in solution. The mechanism of this type of reaction has been demonstrated by the deposition of the Anderson-type heteropolymolybdate $[Al(OH)_6Mo_6O_{18}]^{3-}$ and of Keggin-type aluminotungstic species onto the support during the preparation of MoO_x/γ-Al_2O_3 and WO_x/γ-Al_2O_3 catalysts, respectively.[19] In the present case, degradation of $[Mo_5O_{13}(OMe)_4(NO)]^{3-}$ is followed by the building of a new soluble oxide, $[Mo_5O_{16}(OMe)_2]^{4-}$. This species has not been previously characterized, and it is unlikely that it could exist in an uncomplexed form. However, it is stabilized by coordination to both $\{Mn(CO)_3\}^+$ and Mn^{2+} ions, as shown by the isolation of **6**. The $[Mo_5O_{16}(OMe)_2]^{4-}$ ion is a new member of the family of monovacant Lindqvist-type polyoxomolybdates, besides $[Mo_5O_{13}(OMe)_4(NO)]^{3-}$ and $[Mo_5O_{18}]^{6-}$. This last ion can be seen in the recently reported complex $[\{Ru(\eta^6\text{-}C_6Me_6)\}_2Mo_5O_{18}\{Ru(\eta^6\text{-}C_6Me_6)(H_2O)\}]$.[27] Such species are highly nucleophilic and their isolation is possible only in the presence of stabilizing cations. Possibly the $\{Mn(CO)_3\}^+$ and Mn^{2+} ions do not provide enough stabilization to the $[Mo_5O_{18}]^{6-}$ ion, in contrast to $\{Ru(\eta^6\text{-}C_6Me_6)\}^{2+}$.

Conclusion

The $[Mo_5O_{13}(OMe)_4(NO)]^{3-}$ ion is a multifaceted ligand that offers several coordination sites and can display various coordination modes. In all its previously reported complexes, this anion was linked through terminal oxo ligands as a bidentate, tetradentate, or bridging bisbidentate ligand. Novel coordination modes have been characterized in the course of this work. Indeed, this anion can also provide a triangle of three contiguous bridging oxygen atoms (one oxo and two methoxo groups), thus acting as a κ^3O tridentate ligand. Apparently, side-on coordination can be observed only when terminal coordination is fulfilled. Moreover, the $[Mo_5O_{13}(OMe)_4(NO)]^{3-}/Na^+/Mn(CO)_3^+$ system provides one of the very few examples of isomerization processes involving organometallic cation mobility on polyoxoanions. In addition, the $[Mo_5O_{13}(OMe)_4(NO)]^{3-}$ ion can rearrange under reaction with transition-metal complexes. Degradation of $[Mo_5O_{13}(OMe)_4(NO)]^{3-}$ followed by reaggregation can afford new polyoxoanions, such as $[Mo_5O_{16}(OMe)_2]^{6-}$. In conclusion, the $[Mo_5O_{13}(OMe)_4(NO)]^{3-}$ ion displays a varied coordination chemistry and it provides structural models for surface organometallic chemistry. In that sense, it can be considered as a soluble oxide analogue.

Experimental Section

Materials: The oxonitrosyl precursor $(n\text{Bu}_4\text{N})_2[\text{Na(MeOH)}\{Mo_5O_{13}(OMe)_4(NO)\}]\cdot 3\,\text{MeOH}$ (**1**) was prepared as reported previously.[13] $[MnBr(CO)_5]$ and $[ReBr(CO)_5]$ were prepared as described in the litterature.[33] Reagent grade solvents (methanol and diethyl ether) and inorganic compounds (Br_2, $[Mn_2(CO)_{10}]$, $[Re_2(CO)_{10}]$, $MnBr_2\cdot 4H_2O$, $MnCl_2\cdot 4H_2O$, $Mn(NO_3)_2\cdot 4H_2O$, and $AgNO_3$ were purchased from Strem Chemicals, ACROS, or Aldrich and used as received.

Methods: IR spectra were recorded from KBr pellets on a Bio-Rad Win-IR FTS 165 FT-IR spectrophotometer, and UV-visible spectra were recorded on a Shimadzu UV-2101 spectrophotometer. ^1H and ^{13}C NMR spectra were recorded at 300.13 and 75.47 MHz on a Brucker AC 300 spectrometer. Elemental analyses were performed by the Service Central d'Analyse of the CNRS (Vernaison, France).

Crystal structure analyses: Crystal structure data are summarized in Table 6. Data were recorded at room temperature on either a CAD4 or MACH3 Enraf-Nonius diffractometer with graphite-monochromated

Table 6. Crystal structure data for **2b**, **3**·CH_3OH, **4**, **5a**, and **6**·H_2O

	2b	**3**·CH_3OH	**4**	**5a**	**6**·H_2O
formula	$C_{39}H_{86}Mo_5N_3O_{22}Re$	$C_{63}H_{136}Mo_{10}Mn_2N_5\,NaO_{43}$	$C_{72}H_{172}Mo_{10}MnN_6O_{38}$	$C_{36}H_{84}BrMnMo_5N_3O_{18}$	$C_{74}H_{162}Mn_3Mo_{10}N_4O_{45}$
M_r	1615.0	2744.5	2744.5	1461.0	2958.3
color	red	red	violet	violet	green
space group	$P2_1/c$	$P\bar{1}$	$P\bar{1}$	$P2_1/n$	$P2_1/c$
a [Å]	16.928 (7)	15.037 (7)	12.909 (5)	17.618 (4)	12.659 (4)
b [Å]	17.020 (7)	18.000 (3)	19.136 (6)	18.411 (1)	36.012 (9)
c [Å]	21.857 (10)	21.350 (9)	24.882 (6)	17.641 (10)	25.788 (7)
α [°]		82.72 (2)	68.62 (2)		
β [°]	106.03 (4)	80.04 (4)	82.82 (3)	93.87 (1)	99.13 (3)
γ [°]		65.29 (3)	81.82 (3)		
V [Å^3]	6052 (5)	5160 (3)	5647 (10)	5709 (4)	11607 (6)
Z	4	2	2	4	4
T	ambient	ambient	ambient	ambient	ambient
ρ_{calcd} [g cm^{-3}]	1.77	1.77	1.61	1.70	1.69
μ [cm^{-1}]	30.7	14.5	12.2	20.0	13.90
reflns (unique)	11855	18069	15684	9826	14192
reflns (obsvd)	5697	6278	9339	3504	3968
R (F_o)[a]	6.15	5.11	5.16	6.44	7.82
R_w (F_o)[b]	6.11	5.95	6.26	6.62	7.91
diff peak [e Å^{-3}]	−1.95	−0.82	−0.90	−0.63	−0.86
diff hole [e Å^{-3}]	1.56	0.78	1.03	0.76	1.10

[a] $R=\Sigma||F_o|-|F_c||/\Sigma|F_o|$. [b] $R_w=[\Sigma w(|F_o|-|F_c|)^2/\Sigma w|F_o|^2]^{1/2}$ $(w=w'[1-\{(||F_o|-|F_c||)/6\sigma(F_o)\}^2]^2$ with $w'=1/\Sigma_r A_r T_r(X)$ for which $X=F_c/F_{c(max)}$ with coefficients for a Chebyshev series: 1.29 and 0.73 for **2b**; 4.89, −1.04, and 3.76 for **3**·CH_3OH; 6.44, 0.83, and 4.85 for **4**; 1.15, 0.67, and 0.79 for **5a**; 5.88, −3.68, and 4.19 for **6**·H_2O.

$Mo_{K\alpha}$ radiation ($\lambda = 0.71069$ Å). Crystals of **2b**, **4**, and **5a** were mounted on glass fibers and sealed with an epoxy cement, while crystals of **3**·MeOH and **6**·H_2O were coated with glue and put in Lindeman tubes. Lattice parameters and the orientation matrix were obtained from a least-squares fit of 25 automatically centered reflections in the range 14–14.2° for **2b**, 10–10.5° for **3**·MeOH, 14.9–15° for **4** and **5a**, and 12–12.2° for **6**·H_2O. Intensities were corrected for Lorentz and polarization effects. An empirical absorption correction was applied.[34] Only the reflections with $I > 3\sigma(I)$ were retained for calculations. Data processing was performed with the program CRYSTALS.[35] The structures were solved by direct methods[36] and subsequent Fourier syntheses. All atoms were refined anisotropically, except for **6**·H_2O, for which non-metal atoms were refined isotropically. Hydrogen atoms were not included in the refinements. Neutral-atom scattering factors were used with anomalous dispersion corrections applied.[37] Molecular structures were drawn with the program CAMERON[38] and are reported in Figures 1–5. The numbering scheme for the $\{Mo_5\}$ units in compounds **2b**, **3**·MeOH, **4**, and **5a** follows that previously adopted:[13, 14, 15] the Mo^{II} center was labeled Mo1, while the Mo^{VI} centers were numbered from Mo2 to Mo5. Terminal oxygen atoms (O_t) were labeled O*ii'*, where *i* is the number of the molybdenum atom and *i'* = 1 or 2 depending on whether the oxygen atom is axial or equatorial. Bridging oxygen atoms (O_b) were labeled O*ij*, where *i* and *j* are the indexes of the bridged molybdenum atoms. Finally, the central oxygen atom (O_c) was labeled O10. The numbering scheme for the second distinct $\{Mo_5\}$ unit in **4** was obtained by adding 100 to each basic index. CCDC-193003–193007 contain the supplementary crystallographic data for this paper. These data can be obtained free of charge via www.ccdc.cam.ac.uk/conts/retrieving.html (or from the Cambridge Crystallogrphic Data Centre, 12 Union Road, Cambridge CB2 1EZ, UK; fax: (+44) 1223-336-033; e-mail: deposit@ccdc.cam.ac.uk).

Preparation of (nBu$_4$N)$_2$[Mn(CO)$_3$(H$_2$O){Mo$_5$O$_{13}$(OMe)$_4$(NO)}] (2a): A mixture of $[MnBr(CO)_5]$ (0.140 g, 0.5 mmol) and $AgNO_3$ (0.084 g, 0.5 mmol) in methanol (5 mL) was stirred at room temperature under nitrogen and in the dark for 1 h; afterwards the precipitate of AgBr was filtered off and washed with methanol (2 mL). The light yellow combined filtrates were dropped into a solution of **1** (0.68 g, 0.5 mmol) in deaerated methanol (5 mL), the violet color of which changed at once to orange-red. The solution was stirred in the dark for half of an hour, then its volume was reduced to 5 mL and the solution was allowed to stand at −40 °C for one week. Deep-red air-stable crystals of **2a** were collected by filtration and washed successively with a small amount of cold methanol and diethyl ether. Yield: 0.20 g (27%); IR (KBr): $\tilde{\nu} = 2029$ (s), 1933 (s), 1916 (s), 1617 (s), 1065 (w), 1042 (m), 933 (s), 888 (s), 854 (m), 701 (s), 678 (s), 630 cm^{-1} (m); UV/Vis (MeOH): λ_{max} (ε) = 530 (sh), 410 nm (1930 $mol^{-1}dm^3cm^{-1}$); ^{13}C NMR (75.47 MHz, $CH_3OH/(CD_3)_2CO$, 297 K, TMS): $\delta = 68.4$ (s, 2C; O*C*H$_3$), 68.8 ppm (s, 2C; OC*H*$_3$); elemental analysis (%) calcd for $C_{38}H_{86}MnMo_5N_3O_{22}$: C 31.57, H 5.84, Mn 3.70, Mo 32.33, N 2.83; found: C 31.19, H 6.01, Mn 3.07, Mo 32.96, N 3.21.

Preparation of (nBu$_4$N)$_2$[Re(CO)$_3$(H$_2$O){Mo$_5$O$_{13}$(OMe)$_4$(NO)}] (2b): A mixture of $[ReBr(CO)_5]$ (0.101 g, 0.25 mmol) and $AgNO_3$ (0.042 g, 0.25 mmol) in methanol (5 mL) was stirred for 2 h at room temperature and then filtered. The colorless filtrate was added in a solution of **1** (0.34 g, 0.25 mmol) in methanol (5 mL), and the resulting red solution was refluxed for 24 h. The mixture was filtered while hot, giving a fine white solid, which was discarded, and the filtrate was allowed to stand at −40 °C for 1 d. Red crystals of **2b** suitable for X-ray diffraction were collected by filtration. Further crops of crystals were obtained after concentration of the filtrate under vacuum and prolonged standing at −40 °C. Total yield: 0.1 g (25%); IR (KBr): $\tilde{\nu} = 2013$ (s), 1910 (s), 1885 (s), 1621 (s), 1062 (w), 1041 (m), 936 (s), 885 (s), 852 (m), 698 (s), 672 (sh), 630 cm^{-1} (m); ^1H NMR (300.13 MHz, CD_3OD, 297 K, TMS): $\delta = 4.70$ (s, 6H; OC*H*$_3$), 4.82 ppm (s, 6H; OC*H*$_3$); ^{13}C NMR (75.47 MHz, CH_3OH/CD_3OD, 297 K, TMS): $\delta = 66.4$ (s, 2C; O*C*H$_3$), 66.8 ppm (s, 2C; OC*H*$_3$); elemental analysis (%) calcd for $C_{38}H_{86}Mo_5N_3O_{22}Re$: C 29.00, H 5.37, Mo 29.70, N 2.60, Re 11.53; found: C 28.93, H 5.28, Mo 29.11, N 2.56, Re 11.56.

Preparation of (nBu$_4$N)$_3$[Na{Mo$_5$O$_{13}$(OMe)$_4$(NO)}$_2${Mn(CO)$_3$}$_2$]·MeOH (3·MeOH): Solid $[MnBr(CO)_5]$ (0.140 g, 0.5 mmol) was added to a solution of **1** (0.68 g, 0.5 mmol) in deaerated methanol (10 mL). The resulting red solution was refluxed under nitrogen and in the dark for 16 h, upon which its color had changed to brownish-green. The volume was reduced to 3 mL, and the solution was allowed to stand at −40 °C for one week. Brown crystals with the composition **3**·MeOH, according to crystallography analysis, were collected by filtration. These crystals appeared to be unstable outside the mother liquor due to loss of solvent. Yield: 0.37 g (54%); IR (KBr): $\tilde{\nu} = 2036$ (s), 1930 (s), 1920 (s), 1650 (s), 1030 (m), 1005 (w), 950 (w), 940 (w), 911 (s), 720 (sh), 676 (s), 635 (m), 635 cm^{-1} (sh); UV/Vis (CH_3OH): λ_{max} (ε) = 540 (sh, 134), 390 nm (3850 $mol^{-1}dm^3cm^{-1}$); ^1H NMR (300.13 MHz, CD_3OD, 297 K, TMS): $\delta = 4.59$ (s, 6H; OC*H*$_3$), 5.21 (s, 6H; OC*H*$_3$) ppm; ^{13}C NMR (75.47 MHz, CH_3OH/CD_3OD, 297 K, TMS): 69.2 (s, 2C, O*C*H$_3$), 69.9 (s, 2C, OC*H*$_3$), 221.7 (s, 3C, *C*O); elemental analysis (%) calcd for $C_{62}H_{132}Mn_2Mo_{10}N_5NaO_{42}$: C 27.46, H 4.91, Mn 4.05, Mo 35.38, N 2.58, Na 0.85; found: C 27.29, H 4.95, Mn 3.98, Mo 34.76, N 2.69, Na 0.75.

Preparation of (nBu$_4$N)$_4$[Mn(H$_2$O)$_2${Mo$_5$O$_{13}$(OMe)$_4$(NO)}$_2$] (4): $Mn(NO_3)_2 \cdot 4H_2O$ (0.063 g, 0.25 mmol) and **1** (0.34 g, 0.25 mmol) were added to methanol (10 mL), and the mixture was stirred for 6 h at room temperature. After separation of a fine precipitate, the red filtrate was allowed to stand at −40 °C for one week, after which time the precipitated orange-violet oblong crystals were collected. Yield: 0.115 g (54% based on Mo); IR (KBr): $\tilde{\nu} = 1620$ (s), 1070 (sh), 1046 (m), 927 (s), 897 (s), 862 (m), 696 (br), 625 cm^{-1} (m); UV/Vis (CH_3OH): λ_{max} (ε) = 535 nm (120 $mol^{-1}dm^{-3}cm^{-1}$); elemental analysis (%) calcd for $C_{72}H_{172}MnMo_{10}N_6O_{38}$: C 31.51, H 6.32, Mn 2.00, Mo 34.96, N 3.06; found: C 31.43, H 6.44, Mn 1.91, Mo 32.49, N, 2.99.

Preparation of (nBu$_4$N)$_2$[MnX{Mo$_5$O$_{13}$(OMe)$_4$(NO)}] X = Br (5a), Cl (5b): A mixture of $MnBr_2 \cdot 4H_2O$ (0.72 g, 2.5 mmol) and **1** (3.4 g, 2.5 mmol) in methanol (20 mL) was refluxed for 2 h and then cooled to ambient temperature. Upon addition of diethyl ether (100 mL) to the deep plum-colored solution under vigorous stirring a blue-violet precipitate(**5a**) was obtained. It was recrystallized from methanol due to the possible contamination with (nBu$_4$N)$_2$[Mo_6O_{19}]. Slow diffusion of diethyl ether into the solution of the crude precipitate resulted in the formation of crystals suitable for X-ray diffraction analysis. Compound **5b** was similarly obtained from a mixture of $MnCl_2 \cdot 4H_2O$ (0.215 g, 1.09 mmol) and **1** (1.5 g, 1.09 mmol) in methanol (10 mL).

Compound 5a: Yield after recrystallization: 2.8 g (77%); IR (KBr): $\tilde{\nu} =$ 1643 (s), 1055 (sh), 1035 (s), 938 (s), 868 (s), 845 (s,) 677 (br), 630 cm^{-1} (m); UV/Vis (CH_3OH): λ_{max} (ε) = 545 nm (55 $mol^{-1}dm^3cm^{-1}$); elemental analysis (%) calcd for $C_{36}H_{84}BrMnMo_5N_3O_{18}$: C 29.58, H 5.79, Br 5.47, Mn 3.76, Mo 32.82, N 2.87; found: C 28.99, H 5.66, Br 5.57, Mn 3.72, Mo 32.89, N 2.96.

Compound 5b: Yield after recrystallization: 1.08 g (68%); IR (KBr): $\tilde{\nu} =$ 1645 (s), 1057 (sh), 1033 (s), 938 (s), 870 (s), 846 (s), 678 (br), 630 cm^{-1} (m); UV/Vis (CH_3OH): λ_{max} (ε) = 545 nm (55 $mol^{-1}dm^3cm^{-1}$); elemental analysis (%) calcd for $C_{36}H_{84}ClMnMo_5N_3O_{18}$: C 30.51, H 5.97, Cl 2.50, Mn 3.88, Mo 33.88, N 2.97; found: C 30.54, H 5.95, Cl 2.70, Mn 3.72, Mo 33.10, N 3.00.

Preparation of (nBu$_4$N)$_4$[Mn(H$_2$O)$_2${Mo$_5$O$_{16}$(OMe)$_2$}$_2${Mn(CO)$_3$}$_2$] (6): (nBu$_4$N)$_2$[Mo_2O_7] (0.8 g, 1 mmol) was added to a solution of $Mn(NO_3)_2 \cdot 4H_2O$ (0.05 g, 0.2 mmol) and $[MnBr(CO)_5]$ (0.22 g, 0.8 mmol) in methanol (10 mL). A yellow precipitate was soon apparent. The mixture was refluxed under nitrogen for half an hour, during which time the precipitate became more abundant. The precipitate (analytically pure **6**) was collected by filtration after cooling to ambient temperature. Yield: 0.36 g (61%, based on Mo); IR (KBr): $\tilde{\nu} = 2034$ (s), 1930 (s), 1910 (s), 1000 (m), 950 (m), 933 (s), 910 (s), 895 (sh), 880 (m), 815 (s), 785 (m), 695 (br), 663 (m), 635 cm^{-1} (m); UV/Vis (CH_3OH): λ_{max} (ε) 390 nm (2780 $mol^{-1}dm^3cm^{-1}$); elemental analysis (%) calcd for $C_{74}H_{160}Mn_3Mo_{10}N_4O_{44}$: C 30.29, H 5.50, Mn 5.62, Mo 32.70, N 1.91; found: C 29.52, H 5.13, Mn 5.32, Mo 31.63, N 1.98.

Crystals of **6**·H_2O suitable for X-ray diffraction were obtained in the following way: a mixture of (nBu$_4$N)$_2$[Mo_2O_7] (0.4 g, 0.5 mmol) and $[MnBr(CO)_5]$ (0.27 g, 1 mmol) in methanol (15 mL) was refluxed for 2 h. The mixture was filtered while hot, and the green filtrate was allowed to stand at room temperature for a few days, during which time small green crystals of **6**·H_2O formed together with a yellow powder, which proved to be a mixture of **6** and **7**.

Acknowledgement

We are grateful to the CNRS and to the Université Pierre et Marie Curie for supporting this work.

[1] a) M. T. Pope, *Heteropoly and Isopoly Oxometalates*, Springer, New York, **1983**; b) M. T. Pope, A. Müller, *Angew. Chem.* **1991**, *103*, 56; *Angew. Chem. Int. Ed. Engl*. **1991**, *30*, 34; c) *Chem. Rev*. **1998**, *98*, 1 – 387 (whole issue); d) "Polyoxometalates: From Platonic Solids to Anti-Retroviral Activity": Proceedings of the July 15 – 17, 1992 Meeting at the Center for Interdisciplinary Research in Bielefeld, Germany (Eds.: M. T. Pope, A. Müller), Kluwer, Dordrecht, **1994**; e) "Polyoxometalates: From Synthesis to Industrial Applications": Proceedings of the October 4 – 6, 1999 Meeting at the Center for Interdisciplinary Research in Bielefeld, Germany (Eds.: M. T. Pope, A. Müller), Kluwer, Dordrecht, **2001**.

[2] L. C. W. Baker in *Advances in the Chemistry of Coordination Compounds* (Ed.: S. Kirshner), MacMillan, New York, **1961**, p. 604.

[3] V. W. Day, W. G. Klemperer, *Science* **1985**, *228*, 533.

[4] R. G. Finke, M. W. Droege, *J. Am. Chem. Soc*. **1984**, *106*, 7274.

[5] A. Müller, R. Maiti, M. Schidtmann, H. Bögge, S. K. Das, W. Zhang, *Chem. Commun*. **2001**, 2126.

[6] R. G. Finke in *Polyoxometalates: From Platonic Solids to Anti-Retroviral Activity* (Eds.: M. T. Pope, A. Müller), Kluwer, Dordrecht, **1994**, pp. 267 – 280.

[7] a) C. M. Flynn, Jr., G. A. Stucky, *Inorg. Chem*. **1969**, *8*, 178; b) C. M. Flynn, Jr., G. A. Stucky, *Inorg. Chem*. **1969**, *8*, 332; c) C. M. Flynn, Jr., G. A. Stucky, *Inorg. Chem*. **1969**, *8*, 335; d) B. W. Dale, M. T. Pope, *J. Chem. Soc. Chem. Commun*. **1967**, 792; e) J. M. Buckley, M. T. Pope, *J. Chem. Soc. A* **1969**, 301.

[8] V. W. Day, R. G. Klemperer in *Polyoxometalates: From Platonic Solids* to Anti-Retroviral *Activity* (Eds.: M. T. Pope, A. Müller), Kluwer, Dordrecht, **1994**, pp. 87 – 104.

[9] A. V. Besserguenev, M. H. Dickman, M. T. Pope, *Inorg. Chem*. **2001**, *40*, 2582.

[10] a) H. K. Chae, W. G. Klemperer, V. W. Day, *Inorg. Chem*. **1989**, *28*, 1423; b) H. Hayashi, Y. Ozawa, K. Isobe, *Chem. Lett*. **1989**, 425; c) G. Süss-Fink, L. Plasseraud, V. Ferrand, S. Stanislas, A. Neels, H. Stoeckli-Evans, M. Henry, G. Laurenczy, R. Roulet, *Polyhedron*, **1998**, *17* 2817.

[11] A. M. Landis, Ph.D. dissertation, Georgetown University **1977** (*Diss. Abstr. Int. B* **1979**, *38*, 4225).

[12] a) D. E. Katsoulis, M. T. Pope, *J. Chem. Soc. Chem. Commun*. **1986**, 1186; b) C. L. Hill, R. B. Brown, *J. Am. Chem. Soc*. **1986**, *108*, 536; c) S. Ellis, I. V. Kozhevnikov, *J. Mol. Catal. A* **2002**, *187*, 227.

[13] a) P. Gouzerh, Y. Jeannin, A. Proust, F. Robert, *Angew. Chem.* **1989**, *101*, 1377; *Angew. Chem. Int. Ed. Engl.* **1989**, *28*, 1363; b) A. Proust, P. Gouzerh, F. Robert, *Inorg. Chem.* **1993**, *32*, 5291.

[14] R. Villanneau, A. Proust, F. Robert, P. Gouzerh, *J. Chem. Soc. Dalton Trans.* **1999**, 421.

[15] a) A. Proust, P. Gouzerh, F. Robert, *Angew. Chem.* **1993**, *105*, 81; *Angew. Chem. Int. Ed. Engl.* **1993**, *32*, 115; b) R. Villanneau, A. Proust, F. Robert, F. Villain, M. Verdaguer, P. Gouzerh, *Polyhedron* **2003**, in press.

[16] R. Villanneau, A. Proust, F. Robert, P. Veillet, P. Gouzerh, *Inorg. Chem.* **1999**, 38, 4981.

[17] R. Villanneau, A. Proust, F. Robert, P. Gouzerh, *Chem. Commun.* **1998**, 1491.

[18] a) A. Proust, M. Fournier, R. Thouvenot, P. Gouzerh, *Inorg. Chim. Acta* **1994**, *215*, 61; b) A. Proust, O. Horner, R. Villanneau, P. Gouzerh, *New. J. Chem*. **1996**, *20*, 643.

[19] a) X. Carrier, J.-F. Lambert, M. Che, *J. Am. Chem. Soc*. **1997**, *119*, 10137; b) X. Carrier, J.-B. d'Espinose de la Caillerie, J.-F. Lambert, M. Che, *J. Am. Chem. Soc*. **1999**, *121*, 3377; c) L. Le Bihan, P. Blanchard, M. Fournier, J. Grimblot, E. Payen, *J. Chem. Soc. Faraday Trans*. **1998**, 937.

[20] a) R. H. Reimann, E. Singleton, *J. Chem. Soc. Dalton Trans.* **1974**, 808; b) J. G. Dunn, D. A. Edwards, *J. Organomet. Chem*. **1971**, *27*, 73.

[21] R. Villanneau, R. Delmont, A. Proust, P. Gouzerh, *Chem. Eur. J.* **2000**, *6*, 1184.

[22] a) C. J. Besecker, W. G. Klemperer, *J. Am. Chem. Soc*. **1980**, *102*, 7598; b) C. J. Besecker, V. W. Day, W. G. Klemperer, M. R. Thompson, *Inorg. Chem*. **1985**, *24*, 44.

[23] T. Nagata, M. Pohl, H. Weiner, R. G. Finke, *Inorg. Chem*. **1997**, *36*, 1366.

[24] C. H. Bambord, M. Coldbeck, *J. Chem. Soc. Dalton Trans.* **1978**, 4.

[25] V. W. Day, M. F. Fredrich, M. R. Thompson, W. G. Klemperer, R.-S. Liu, W. Shum, *J. Am. Chem. Soc.* **1981**, *103*, 3597.

[26] a) J. Besecker, V. W. Day, W. G. Klemperer, M. R. Thompson, *J. Am. Chem. Soc*. **1984**, *106*, 4125; b) K. Nomiya, C. Nozaki, M. Kaneko, R. G. Finke, M. Pohl, *J. Organomet. Chem*. **1995**, *505*, 23.

[27] V. Artero, A. Proust, P. Herson, P. Gouzerh, *Chem. Eur. J.* **2001**, *7*, 3901.

[28] a) D. J. Edlund, R. J. Saxton, D. K. Lyon, R. G. Finke, *Organometallics* **1988**, *7*, 1692; b) M. Pohl, Y. Lin, T. J. R. Weakley, K. Nomiya, M. Kaneko, H. Weiner, R. G. Finke, *Inorg. Chem*. **1995**, *34*, 767; c) V. W. Day, T. A. Eberspacher, W. G. Klemperer, R. P. Planalp, P. W. Shiller, A. Yagasaki, B. Zhong, *Inorg. Chem*. **1993**, *32*, 1629.

[29] M. Abe, K. Isobe, K. Kida, A. Yagasaki, *Inorg. Chem*. **1996**, *35*, 5114.

[30] V. Artero, A. Proust, P. Herson, R. Thouvenot, P. Gouzerh, *Chem. Commun*. **2000**, 883.

[31] a) M. Pohl, R. G. Finke, *Organometallics* **1993**, *12*, 1453; b) D. Attanasio, F. Bachechi, L. Suber, *J. Chem. Soc. Dalton Trans.* **1993**, 2373, c) Y. Hayashi, F. Müller, Y. Lin, S. M. Miller, O. P. Anderson, R. G. Finke, *J. Am. Chem. Soc*. **1997**, *119*, 11401.

[32] S. L. Scott, P. Dufour, C. C. Santini, J.-M. Basset, *Inorg. Chem*. **1996**, *35*, 869.

[33] a) E. W. Abel, G. Wilkinson, *J. Chem. Soc. A* **1959**, 1501; b) S. P. Schmidt; W. C. Trogler, F. Basolo, *Inorg. Synth*. **1990**, *28*, 162.

[34] N. Walker, D. Stuart, *Acta Crystallogr. Sect. A* **1983**, *39*, 158.

[35] D. J. Watkin, J. R. Carruthers, P. W. Betteridge, CRYSTALS, Chemical Crystallography Laboratory, University of Oxford, **1996**.

[36] G. M. Sheldrick, SHELXS86, Program for the Solution of Crystal Structures, University of Göttingen, **1986**.

[37] *International Tables for X-ray Crystallography, Vol. IV*, Kynoch, Birmingham, **1974**.

[38] L. J. Pearce, D. J. Watkin, CAMERON, Chemical Crystallography Laboratory, University of Oxford, **1996**.

Received: November 4, 2002 [F4547]